Journal of Optoelectronics and Biomedical Materials Vol. 6 Issue 4, October-December 2014 p. 119-129

SOL-GEL DERIVED Mg AND Ag DOPED ZnO THIN FILM ON GLASS SUBSTRATE : STRUCTURAL AND SURFACE ANALYSIS

S. SHANMUGAN[*], D. MUTHARASU, I. ABDUL RAZAK
Nano Optoelectronics Research Laboratory, School of Physics,
Universiti Sains Malaysia (USM), 11800, Minden, Pulau Pinang, Malaysia.

Metal (Ag and Mg) doped ZnO thin film was prepared by sol-gel spin coating method on glass substrates followed by annealing at 4 different temperatures (300 to 450°C) to understand the structural behavior. The structural analysis of Mg doped ZnO thin film was showed the crystal grown in their preferred hexagonal (100) orientation. The crystallinity of Ag doped ZnO thin film was poor as compared with as grown and Mg doped ZnO thin film. Only hexagonal structure was observed with Mg doped ZnO thin film. From the atomic force microscopy (AFM) images, nanocrystalline structure was noticed with doped ZnO thin film and nano-plate like structure was observed from Ag doped ZnO thin film at 350°C temperature. Noticeable change in surface morphology was observed from the Ag and Mg doped ZnO thin film when annealed at the range from 300 to 400 °C. Surface roughness value was increased for Ag doped ZnO thin film annealed at above 400°C. Annealing temperature showed immense effect on surface morphology as well as grain size of both Ag and Mg doped ZnO thin film as compared with bare ZnO thin film. Fourier Transform Infra-Red spectrometer (FTIR) spectra showed the ZnO related peaks with very low intensity. The FTIR spectra revealed the influence of metal doping to ZnO as well as annealing.

(Received September 30, 2014; Accepted November 20, 2014)

Keywords: ZnO thin film, Spin coating, Doping, Surface properties, Structural properties

1. Introduction

The development of nanoscience and nanotechnology research on ceramic materials shows a lot of promising applications of ZnO in the manufacturing of nanoscale-based electronic and optoelectronic devices, because of its abundance, nontoxicity, and the fact that it is a wide band gap (3.2–3.3 eV) semiconductor with good carrier mobility. Furthermore, it can also be doped both n-type and p-type [1-4].

The main motivations behind crafting materials at smaller dimensions have been to increase the surface-to-volume ratio and to reduce diffusion path length. Dopants are critically important for making nano-devices. Tiny amounts of dopants that act as donors/acceptors are introduced into the semiconductor crystal lattice to affect significant changes in semiconductors [5]. The doping of transition metals induces more mismatches and defects in the lattice structure of ZnO. The intrinsic oxygen defects influences appreciable photoluminescence (PL) and magnetic properties. Mg doped ZnO is a II–VI semiconductor alloy which has a wide band gap from 3.36 eV of ZnO up to about 6.7 eV with the inclusion of Mg [6,7].

Particularly in high efficiency Cu(In, Ga)Se2 (CIGS)–based solar cells, Mg doped ZnO is regarded as a promising buffer layer for the replacement of toxic CdS not only for environmental problems but also the advantage that the conduction band offset between buffer layer and absorber material can be controlled properly using its tunable band gap energy [8,9]. Ko and Yu [10] synthesized Ag doped ZnO nanorod arrays and found that Ag incorporation can greatly increase the optical absorption. Later, Fenglin Xian et al. [11] prepared Ag doped ZnO thin film by spin

---

[*] Corresponding author: shagan77in@yahoo.co.in

coating method and reported the 4% Ag doped ZnO thin film showed improved absorption with solar cell's energy conversion efficiency improvement of 2.47%.

There are various methods for preparing metal doped ZnO thin films such as sol gel, spin coating, dip coating, spray pyrolysis, chemical bath deposition, pulsed laser deposition, sputtering. The sol–gel spin coating method has distinct advantages such as cost effectiveness, thin, transparent, multicomponent oxide layers of many compositions on various substrates, simplicity, excellent compositional control, homogeneity and lower crystallization temperature [12]. Sol gel process has the unique advantages of allowing the preparation of materials of the same composition in different physical forms, coating by varying experimental conditions.

In this study, Ag and Mg doped ZnO thin film is prepared on glass substrates by sol-gel rout followed by spin coating method. The prepared samples are annealed for various temperatures to analyze the influence of temperature on structural, surface and optical properties as well. The observed results are discussed and reported.

2. Experimental methods

Nanostructured bare and Mg and Ag doped ZnO thin films were deposited onto glass substrates by sol–gel spin coating method. For sol-gel preparation, Zinc acetate dehydrate (ZnAc) was used as Zn source material. In addition, 2-butanol and diethanolamine (DEA) were used as solvent and stabilizer respectively. To prepare the starting solution for bare ZnO thin film deposition, 0.4 M ZnAc was dissolved in 2-butanol and prepared the ZnAc solution with DEA solution and the molar ratio of DEA to ZnAc was kept at 1.0. The mixture was stirred at 70°C using a magnetic stirrer until a clear and homogeneous solution formed.

In order to dope the Mg and Ag elements to ZnO, $MgCl_2$ and $AgNO_3$ were selected as a source material. For Ag doping, ZnAc was dissolved in 15 ml of isopropanol and added DEA solution under continuous stirring by magnetic stirrer at room temperature (solution A). $AgNO_3$ solution was mixed with 10 ml of isopropanol and added to the clear solution of ZnAc (solution A). The expected weight ratio of Ag/Zn is 7% for this work. For Mg doping, ZnAc solution (solution A) is mixed with $MgCl_2$ tetradihydrate (2% Wt.) dissolved in 25 ml of ethanol followed by the addition of 2.52 ml of DEA solution to get clear solution.

The prepared solutions were used to coat bare, Mg and Ag doped ZnO thin film by spin coating unit. Before coating, the microscope glass substrates were cut into several pieces with 2 cm x 2 cm dimensions and cleaned with soap solutions followed by rinsing using distilled water. Later, the substrates were dipped in ethanol for 10 min in an ultrasonic bath followed by acetone cleaning. Finally, the cleaned substrates were dried in hot air oven for deposition. The dried substrates were fixed on the center of the spin coater using a double sided tape. 5 drops of the prepared solution was put at the center of the class substrate by plastic dropper and switched on the spinning motor. The rotating disc speed was controlled and maintained as 3000 rpm, 2000 rpm and 3000 rpm for bare ZnO, Ag doped ZnO and Mg doped ZnO respectively. The spinning time for all coating was fixed as 30 seconds. The coating cycles for bare ZnO, Ag doped ZnO and Mg doped ZnO thin film was fixed as 20, 15 and 10 respectively. Depending on the wet quality of the film, the drying time was varied from 1 min to 10mins and temperature was changed from 100°C to 150°C respectively. Finally, annealing process was also employed in air using tube furnace for about 1 hr at various temperatures from 300°C to 450°C at 50°C step size.

The structural properties of the film were tested by high resolution x-ray diffraction analysis (HRXRD, X'pert-PRO, Philips, Netherlands) and the results are compared and indexed using JCPDS data. A CuKα (λ = 1.54056 Å) source was used, with a scanning range between 2θ = 20° and 65°. This range has been selected because of most of ZnO peaks were observed between this ranges. The surface morphology of the prepared samples was tested by the atomic force microscope (model: ULTRA Objective, Surface Imaging Systems, GmbH) in the non-contact mode. The surface roughness and the particle size were analyzed by using nanoscope surface analysis software. For the chemical composition analysis, the fourier transform infrared spectroscopy (FTIR) was used to analyze our bare and doped ZnO thin film samples by recording the transmittance spectra of all samples.

3. Results and discussion

3.1 Structural analysis

The X-ray diffraction spectra of spin coated Ag and Mg doped ZnO thin films on glass substrates are shown in fig. 1. It is observed that the ZnO film doped with Ag shows amorphous structure with few hexagonal phases of ZnO. Since the glass substrate is an amorphous material, the particles should be randomly oriented; correspondingly, the crystals were also randomly oriented in the form of thin film [13]. Figure 1 clearly shows that the prepared bare and metal doped ZnO thin films have nano crystalline structure and polycrystalline nature [14].

From fig.1, it is also noticed that the hydroxide compound of Zn ($Zn(OH)_2$) is also exist and shows the dominated x-ray diffraction peak for all Ag doped samples with irrespective to the annealing temperatures. It may be attributed to the effect of Ag doping into ZnO and the influence of Ag presence in the ZnO structure since these hydroxide peaks are not observed with Mg doped ZnO thin film samples.

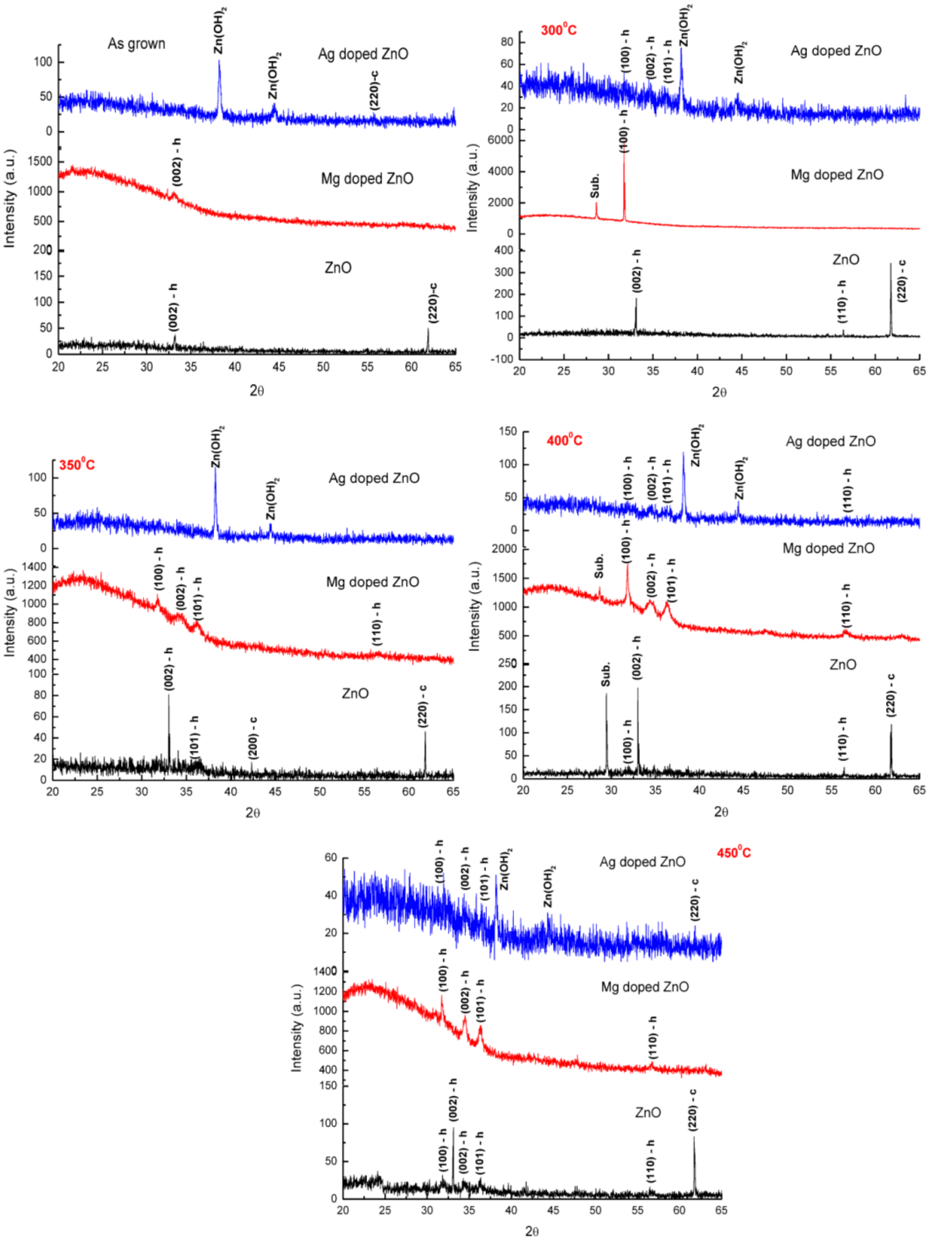

Fig. 1 XRD spectra of sol-gel derived as grown, Ag and Mg doped ZnO thin film for various annealing temperatures.

It is also observed that the hexagonal phase of ZnO with different orientations could also be observed for the samples annealed at 300 °C, 400 °C and 450 °C except for the sample annealed at 350°C. Presence of several peaks in all the thin films indicates random orientation of the crystallites and hence the maximization of surface energy and internal stress are possible with the undoped and doped ZnO thin film [15]. For comparison, the xrd spectra of bare and annealed ZnO thin film are also recorded and plotted with xrd spectra of Ag and Mg doped ZnO thin film as shown in fig. 1. It clearly indicates the influence of metal doping on the structural phase change of ZnO thin film. It also clearly indicates the absence of alloy thin film formation as a result of doping. It is evident from the xrd pattern that no extra peaks related to Mg, Ag, other oxides or any Ag-Zn alloy or Mg-Zn alloy phase are observed. It is indicating that as synthesized Mg doped ZnO samples (as grown and annealed at 300°C) are single phase. These obtained results indicated that the metal doping is occurred effectively into the ZnO lattice.

From fig.1, in as grown films, the mixed phases (hexagonal and cubic) are noticed for bare ZnO thin film and Mg doped ZnO thin film. As grown ZnO film shows the cubic ZnO phase with (220) orientation which is having strong intensity. The (002) plane of ZnO has the minimum surface free energy [16], so most of the films show the observation of (002) oriented peaks (namely, the *c*-axis direction), in addition with other directions.

As stated in the above paragraph, only Zn $(OH)_2$ peaks are observed from the Ag doped ZnO thin film and no hexagonal phases are observed. In order to test the influence of heat on the characteristics (structural and surface morphology) of bare and doped ZnO thin film, the samples are annealed at various temperatures from 300 to 450 °C and the XRD spectra are recorded for the same. The fig.1 is also showing the effect of annealing clearly and noticeable changes on structural properties could be observed. Fig.1 clearly shows that the annealing process suppress the growth of (220) oriented cubic ZnO phase in presence of metal (Mg and Ag) in ZnO lattice. It is the evidence of crystal defects in presence of metal in the ZnO crystal lattice. At 300 °C, a strong peak with high intensity is observed and indexed as (100) hexagonal phase for the Mg doped ZnO thin film. A decrease in intensity of this (100) phase is also noticed when the annealing temperature is increased. Moreover, additional phase’s related to hexagonal with (002), (101) and (110) orientations are also observed for the bare ZnO and Mg doped ZnO thin films as the temperature increases from 300 °C to 450 °C. These phases are also noticed for Ag doped ZnO thin film with very low intensity when the samples are annealed at above 400°C.

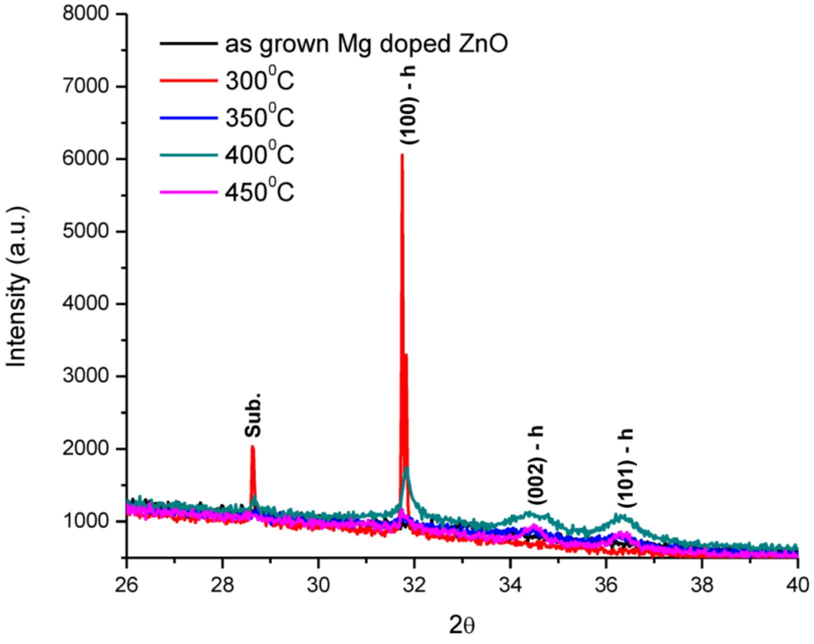

Fig. 2 XRD spectra of Mg doped ZnO thin film annealed at various temperatures

From these observations, the Ag and Mg elements were influenced the structural phase formation and the crystallinity of ZnO thin film prepared by spin coating process. According to Scherrer’s formula, (D =0.9/FWHM cos θ, where D is the average grain size, FWHM is the full, wide, at a hall maximum, and θ is the grades at 2θ), the peak width of each diffraction spectra is the indication of crystallite size and the crystallite size increases as the peak width decreases which could be possible at high annealing temperatures. Contrarily, the crystallite size decreases as the annealing temperature increases for Mg doped ZnO thin film. This could be verified by studying the peak intensity as well as width analysis. For peak intensity analysis, the XRD spectra of Mg doped ZnO thin film annealed at various temperatures is plotted in the same figure as shown in Fig.2. It clearly shows that the intensity reduces noticeably as the annealing temperature increases and also the crystallite size too (observed the broadening of peak). It is believed that the annealing temperatures help to make a good bond between the ZnO and Mg and possible for deterioration in the film crystallinity [17].

The width of the peak drastically increases for the sample annealed at above 350°C and expected to the formation of nano crystal at temperature especially for 400°C since a very broad peak is noticed with the sample annealed at 350 °C. It is indirectly says the poor crystallinity which is against the results published by Zhao-Hui Li et al [17]. Even though the Mg doped into ZnO lattice, there is not much difference in XRD peak positions for both as grown and annealed samples. This is because of the ionic radii of Zn^{2+} (0.60 Å) and Mg^{2+} (0.57Å) are almost same and suggested that the Mg doped ZnO thin film has the nearly same phase as the pure ZnO film [17].

3.2 Surface analysis

The surface morphology of spin coated metal doped ZnO thin film on glass substrates are recorded by atomic force microscopy and the images are given in Fig.3, Fig.4, Fig.5, Fig.6 and Fig.7. From these figures, it clearly indicates the influence of both annealing temperature as well as the doping metal on the surface morphology of the samples. The glass substrates were completely covered with different sizes of nanoparticles and the doping element significantly affects the surface morphology of the films noticeably.

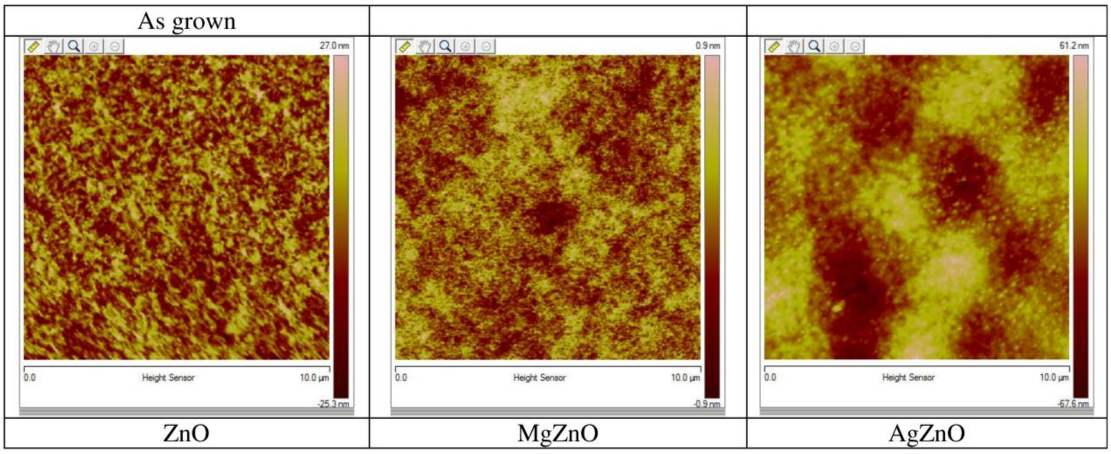

Fig. 3 SEM images of undoped, Ag and Mg doped ZnO thin film by spin coating method.

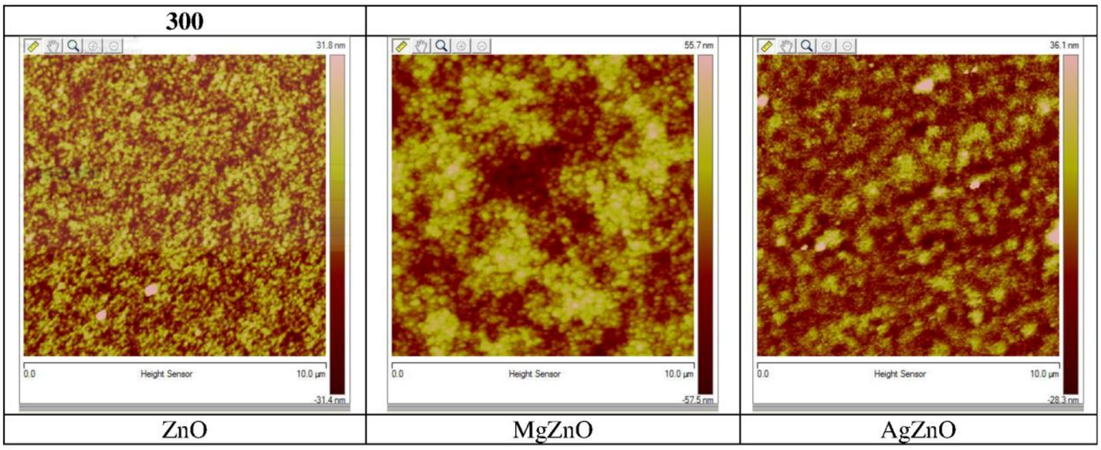

Fig. 4 SEM images of 300 ° C annealed undoped, Ag and Mg doped ZnO thin film by spin coating method.

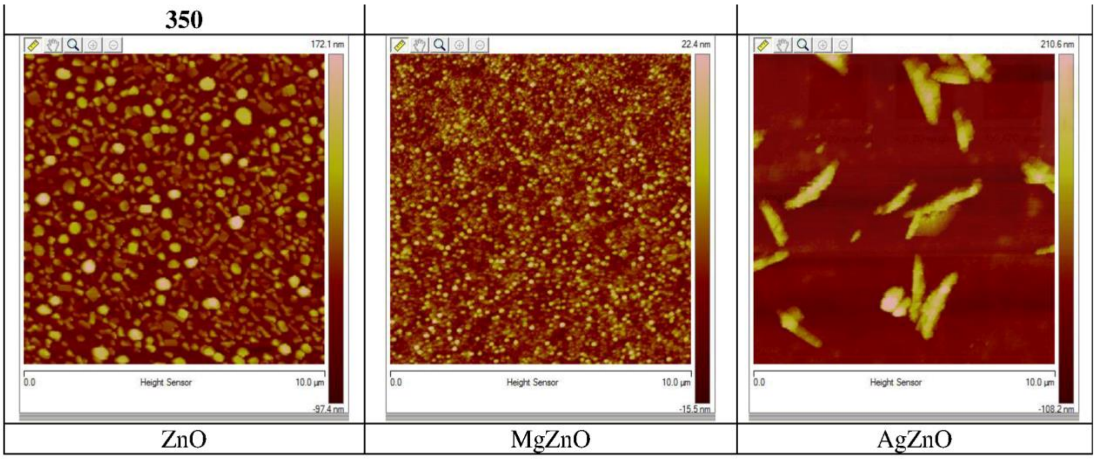

Fig. 5 SEM images of 350 ° C annealed bare, Ag and Mg doped ZnO thin film by spin coating method.

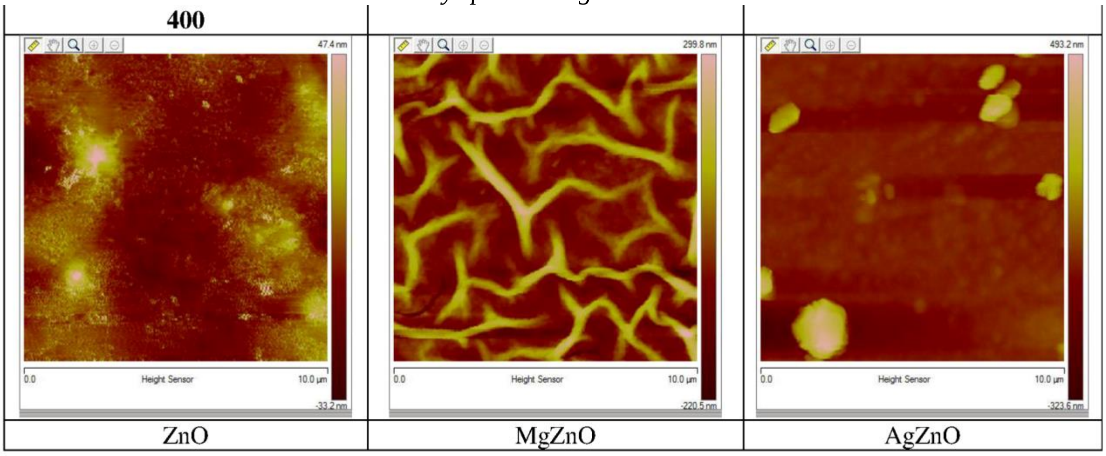

Fig. 6 SEM images of 400 ° C annealed bare, Ag and Mg doped ZnO thin film by spin coating method.

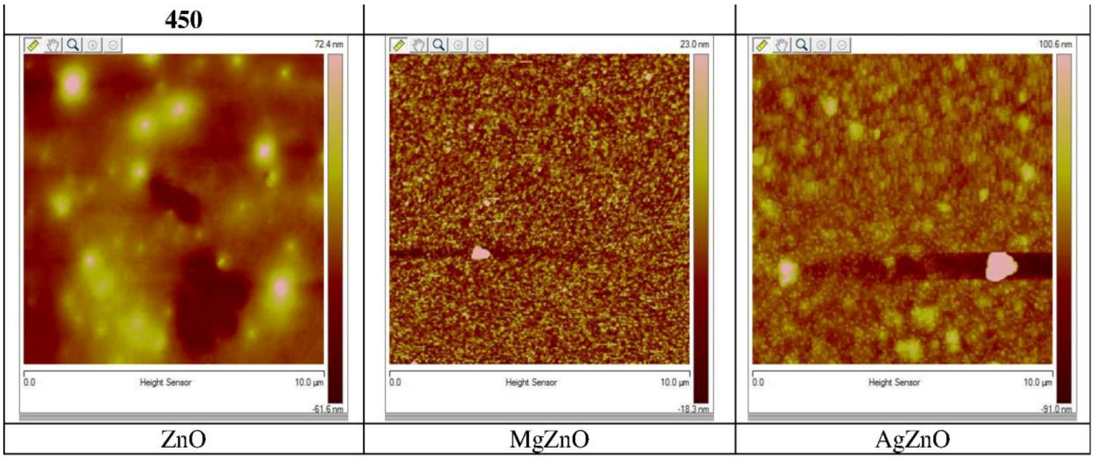

Fig. 7 SEM images of 450 ° C annealed undoped, Ag and Mg doped ZnO thin film by spin coating method.

The morphology of a particle depends on the value of ionic fraction of the bond. Therefore, result can be explained on the basis of ionic fraction of the bond in Mg and Ag doped ZnO. On Pauling scale, the electronegativity of Zn, Mg and Ag is 1.65, 1.31 and 1.93 on same scale respectively i.e. ionic fraction is low (~1) that leads to longitudinal structures [18,19]. These results reveal that the morphology of the parent compound changes by doping element.

From the results of un-annealed samples, the metal doping affects the surface morphology noticeably and observed porous like structure for Ag doped ZnO thin film. It also reveals the less density surface for Mg doped ZnO thin film and it is expected for increased electrical resistivity [20]. As we know, the annealing process has immense effect on surface morphology and also observed interesting changes on surface morphology. Especially for samples annealed at 350 °C from our study (fig. 5), surface of Mg doped ZnO thin film has the surface with loosely bounded nano particles. But a noticeable change in surface morphology is achieved for Ag doped ZnO thin film samples for the same temperature (350°C). It reveals the nano plates like structure on the surface of Ag doped ZnO thin film surface. At 400°C (fig.6), a noticeable change in surface morphology is achieved for doped samples.

A wave like nematic structure is also noticed with Mg doped samples where the sample did not have single uniform direction across its whole volume but instead the surface was broken into smaller, differently oriented regions and a uniform surface is also observed for Ag doped samples. It is attributed that there is a certain degree of influence of Mg^{2+} ion on the growth kinetics during the thin film deposition process [21].

A uniform surface morphology with nano particles is also observed for Mg doped and Ag doped ZnO thin film. But particle agglomeration is noticed with the Ag doped ZnO thin film. Overall, a distinct change on surface morphology of ZnO is observed as a result of doping considerably. In order to study the surface properties in detail, the surface roughness factor and the particle size of undoped and doped ZnO thin film is evaluated by surface analysis software and the observed results are summarized in table – 1.

Table .1 Average surface roughness (R_a) and particle size of as grown and doped ZnO thin film for various annealing temperatures.

Glass	**As grown**		**300°C**		**350°C**		**400°C**		**450°C**	
	R_a		R_a		R_a		R_a		R_a	
Bare ZnO	6	286	7.3	331	32.4	322	8.4	558	12.2	588
MZO	2.5	404	13.3	527	38.8	243	60.5	1127	4.5	439
AZO	14.4	450	6.7	335	25.4	809	38.4	854	13.2	662

* all values are in nanometer scale

It reveals that the surface roughness and the particle size are changed drastically with respect to doping and also the annealing temperatures. From the table - 1, Mg doping to ZnO increases the surface roughness for all annealed temperatures except for as grown condition. A drastic decrease in surface roughness as well as very low value of 0.25 nm could be observed for Mg doped ZnO thin film in as grown condition. The surface roughness increases for Mg doped ZnO thin film as the annealing temperature increases until 400 °C. This change in surface roughness may be due to the grain growth during thermal annealing process. This can be regarded as the merging process of ZnO nanoparticles induced from thermal annealing. In the case of ZnO nanoparticles, at a higher temperature, the zinc or oxygen defects at the grain boundaries favor the merging process by stimulating the coalescence of more grains during annealing [22].

For Ag doped ZnO thin film, the change in surface roughness is not stable and up & down behavior in roughness value is also noticed as the annealing temperature increases when compare to as grown ZnO thin film. As compared with Mg doped ZnO thin film, the Ag doping process decreases the surface roughness noticeably for ZnO thin film as the annealing temperature increases from 300 to 400°C. On considering the average particle size, a gradual increase in particle size is achieved with as grown samples as a result of doping. As a result of more energy available during the annealing process, the atoms may diffuse and occupy the correct site in the crystal lattice and grains with lower surface energy will grow larger at higher temperatures [23]. Li et al. reported that the grain size of the film gradually decreases as the Mg content increases [17]. Contrarily, in our study, the Mg doping to ZnO increases the particle size of ZnO thin film noticeably when annealed at 300°C and 400°C especially for the samples annealed at 400°C (1.127 μm), even though the atomic size of Mg metal is smaller than Ag atom. It may be the evidence for the reduced electrical resistivity [20]. The particle size of Ag doped ZnO thin film shows high value as compared with bare ZnO thin film at as grown condition and all annealing temperatures.

3.3 FTIR analysis

It is the combination of all data that helps us to understand, analyze, and refine more effectively the structure of films. The frequencies at which absorption occurs may indicate the type of functional groups present in the substance. The FTIR transmittance spectra of bare and metal doped ZnO thin film before and after annealing are recorded at room temperature as shown in Fig.8. It reveals that the metal doping influence the optical behavior of ZnO thin film. A sharp absorption band noticed in between 440–455 cm^{-1} indicates the vibrational properties of ZnO for Mg doped ZnO thin film samples. The stretching vibrational mode around ~415 cm^{-1} is the IR active E1 (TO) mode of wurtzite ZnO and it was attributed to the Zn–O stretching vibration for tetrahedral surrounding of zinc atoms. The peak around 454cm-1 and 580 cm-1 may be attributed to E2 (LO) and E1 (LO) mode typical for ZnO wurtzite structure [24].

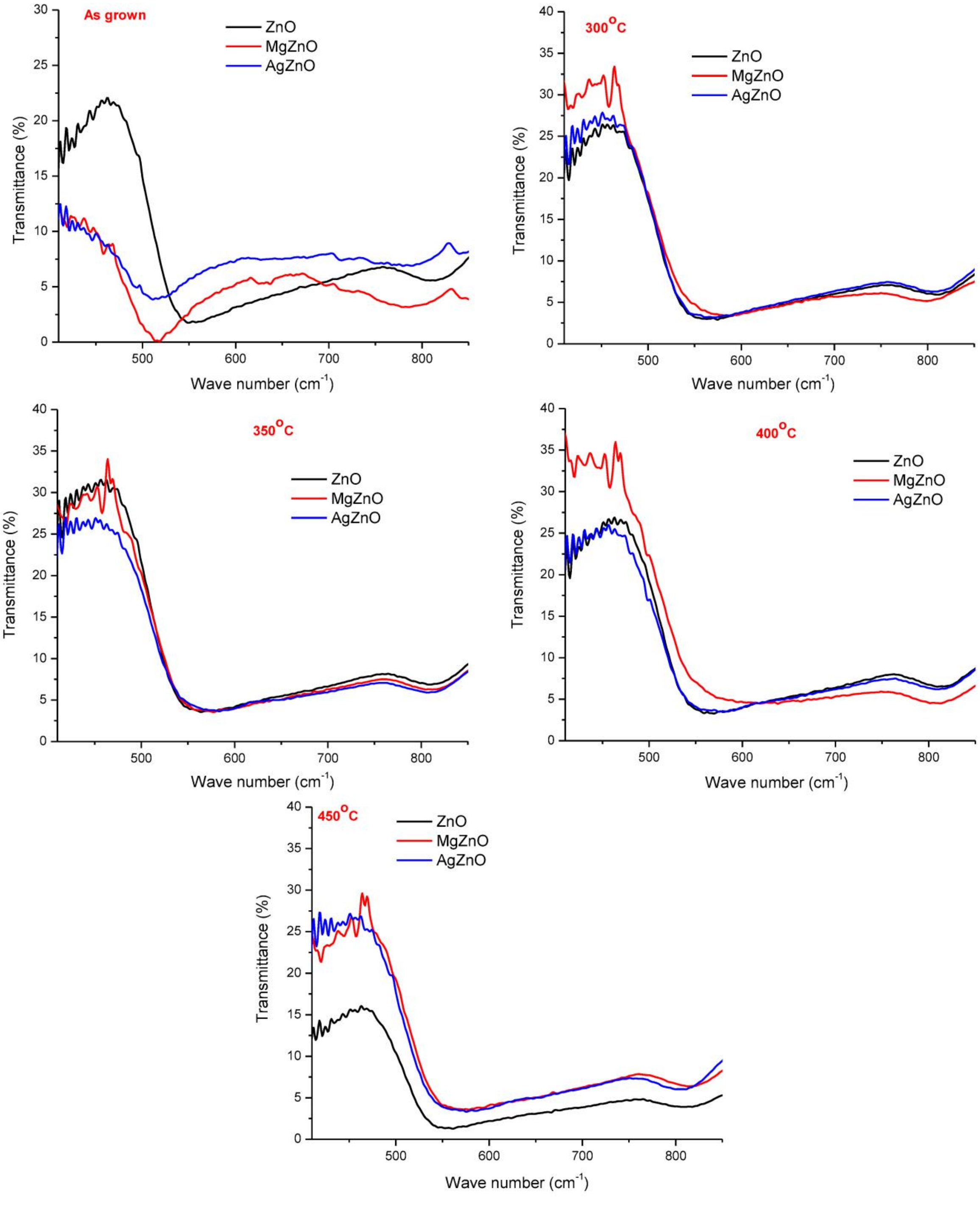

Fig. 8 FTIR spectra of sol-gel derived ZnO thin film before and after doping with Ag and Mg.

Common bands exist in all cases, such as the broad OH band, C–H stretching vibrations etc. and they are not considered here for discussion. In as grown film, a broad absorption peak at around 514 cm^{-1} is noticed which is related to Mg-O vibrations [25]. But this MgO peak was not evidenced by XRD analysis. This peak could not be identified for Mg doped ZnO thin film after annealing process. A sharp peak at 457 cm-1 is noticed for all Mg doped ZnO thin film and the intensity of peak changes with respect to the annealing temperatures and high intensity is observed with the samples annealed at 400°C. These kinds of observations have not been noticed for bare and Ag doped ZnO thin film before and after annealing process.

4. Conclusions

Mg and Ag doped ZnO thin films were synthesized on glass substrates using sol-gel spin coating method. Preferred (100) oriented hexagonal phase of ZnO was confirmed for all samples especially Mg doped ZnO thin film showed high intensity peak. The crystallinity of Ag doped ZnO thin film was poor even though the annealing temperature increased upto 450°C. Nano platelets like structure was noticed with Ag doped ZnO thin film annealed at 350°C. Annealing temperature also influenced the surface morphology irrespective to the doping element and low surface roughness was noticed with Mg doped ZnO thin film in as grown as well as annealed at 450°C. FTIR spectra was also evidenced for Mg doping to ZnO and also showed the effect of annealing for all as grown and annealed samples.

Acknowledgement

The authors express their gratitude for the FRGS project (203/PFIZIK/6711350) that provides the fund to carry out the research work successfully in school of physics. In addition, the authors would like to acknowledge for the use of research facilities such as spin coating machine, FESEM, FTIR etc., available in NOR Lab, School of Physics, Universiti Sains Malaysia.

References

[1] S. Y. Lee, E. S. Shim, H. S. Kang, S. S. Pang, and J. S. Kang, Thin Solid Films **473**, 31 (2005).
[2] Y. J. Zeng, Z. Z. Ye, W. Z. Xu et al., Journal of Crystal Growth, **283**, 180 (2005).
[3] H. S. Kang, B. D. Ahn, J. H. Kim et al, Applied Physics Letters, 88, Article ID 202108, (2006).
[4] B. Yao, D. Z. Shen, Z. Z. Zhang et al., Journal of Applied Physics, 99, Article ID12351, (2006).
[5] Manikandan E, Moodley MK, Krishnan R. J Nanosci Nanotechnol, **10**, 5602 (2010)
[6] T. Gruber, C. Kirchner, R. Kling, F. Reuss, A. Waag, Appl. Phys. Lett. **84**, 5359 (2004).
[7] A.K. Sharma, J. Narayan, J.F. Muth, C.W. Teng, C. Jin, A. Kvit, R.M. Kolbas, O.W. Holland, Appl. Phys. Lett. **75**, 3327 (1999).
[8] I. Lauermamn, Ch. Loreck, A. Grimm, R. Klenk, H. Monig, M.Ch. Lux-Steiner, Ch.H. Fischer, S. Visbeck, T.P. Niesen, Thin Solid Films **515**, 6015 (2007).
[9] T. Torndahl, C. Platzer-Bjorkman, J. Kessler, M. Edoff, Prog. Photovolt. Res. Appl. **15**, 225 (2007).
[10] Y.H. Ko, J.S. Yu, Phys. Status Solidi (a) **208**, 2778 (2011).
[11] F. Xian, K. Miao, X. Bai, Y. Ji, F. Chen, X. Li, Optik **124**, 4876 (2013).
[12] M. Caglar, S. Ilican, Y. Caglar, F. Yakuphanoglu, Applied Surface Science **255**, 4491 (2009).
[13] J. A. Alvarado, A. Maldonado, H. Juarez, and M. Pacio, . Journal of Nanomaterials, Volume 2013, Article ID 903191, 9 pages, http://dx.doi.org/10.1155/2013/903191
[14] Caglar et al. Appl. Surf. Sci. **255**, 4491 (2009)
[15] D. Bao, H. Gu, A. Kuang, Thin Solid Films **312**, 37 (1998).
[16] N. Fujimura, T. Nishihara, S. Goto, J. Xu, and T. Ito, Journal of Crystal Growth 130, 269 (1993).
[17] Zhao-Hui Li, Eou-Sik Cho, Sang Jik Kwon, Appl. Surf. Sci. **314**, 97 (2014)
[18] C Wu, L Shen, Y Zhag, Q. Huang Mater Lett **65**, 1794 (2011)
[19] Ü Özgür, YI Alivov, C Liu, A. Teke J Appl Phys, **98**, 041301 (2005).
[20] Davood Raoufi, Taha Raoufi, Appl. Surf. Sci. **255**, 5812 (2009)
[21] G. Vijayaprasath, R. Murugan, G. Ravi, T. Mahalingam, Y. Hayakaw, Appl. Surf. Sci. **313**, 870 (2014)
[22] A.V. Dijken, E. Meulenkamp, D. Vanmaekelbergh, A. Meijerink, J. Phys. Chem.

B **104**, 1715 (2000).
[23] Z.B. Fang, Z.J. Yan, Y.S. Tan, Appl. Surf. Sci. **241**, 303 (2005).
[24] E.M. Bachari, G. Baud, S. Ben Amor and M. Jacquet, Thin Solid Films, **348**, 165 (1999).
[25] Mehran Rezaei, Majid Khajenoori and Behzad Nematollahi, Powder technol. **205**, 112 (2011).